

Finite-Temperature QCD on the Lattice

Akira Ukawa^a

^aInstitute of Physics, University of Tsukuba, Tsukuba, Ibaraki 305, Japan

Recent developments in finite-temperature studies of lattice QCD are reviewed. Topics include (i) tests of improved actions for the pure gauge system, (ii) scaling study of the two-flavor chiral transition and restoration of $U_A(1)$ symmetry with the Kogut-Susskind quark action, (iii) present understanding of the finite-temperature phase structure for the Wilson quark action. New results for finite-density QCD are briefly discussed.

1. Introduction

Finite-temperature studies of lattice QCD have been pursued over a number of years. Quite clearly the pure gauge system is the best understood of the entire subject. The system has a well-established first-order deconfinement transition[1], and extensive and detailed results are already available for a number of thermodynamic quantities[2]. Nonetheless many new studies have been made for this system recently. The purpose is to examine to what extent cutoff effects in thermodynamic quantities are reduced for improved actions as compared to the plaquette action which had been used almost exclusively in the past.

Full QCD thermodynamics with the Kogut-Susskind quark action has also been investigated extensively in the past. A basic question for this system is the order of chiral phase transition for light quarks. For the system with two flavors, finite-size analyses carried out around 1989-1990 indicated an absence of phase transition down to the quark mass $m_q/T \approx 0.05$ [3], and a more recent study[4] attempted to find direct evidence for the second-order nature of the transition, as suggested by the sigma model analysis in the continuum[5], through scaling analyses. Scaling studies have been continued this year to establish the universality nature of the transition on a firm basis. Another issue discussed at the Symposium is the question of restoration of $U_A(1)$ symmetry at the chiral transition. Results have been presented for equation of state both without and with use of improved actions.

Studies of thermodynamics with the Wilson

quark action is much less developed compared to that for the Kogut-Susskind quark action. Past simulations found a number of unexpected features, which made even an understanding of the phase structure a non-trivial problem[6]. Recently, however, considerable light has been shed on this problem through an analysis based on the view that the critical line of vanishing pion mass marks the point of a second-order phase transition which spontaneously breaks parity and flavor symmetry[7]. Some new work with improved actions, which was initiated a few years[8], has also been made this year.

In this article we review recent studies of finite-temperature lattice QCD. In Sec. 2 we summarize results for the pure gauge deconfinement transition obtained with a variety of improved actions. Results for the two-flavor chiral transition for the Kogut-Susskind quark action are discussed in Sec. 3 with the main part devoted to scaling analyses of the order of the transition. In Sec 4 we describe recent progress on the phase structure analysis for full QCD with the Wilson quark action. This year's results for finite density are briefly discussed in Sec 5. Our summary and conclusions are presented in Sec. 6.

2. Recent work on pure gauge system

In Table 1 we list recent studies of the pure gauge system using improved actions. Among actions constructed through renormalization group, RG(1,2)[18] includes 1×2 loop in addition to the plaquette. The action FP is an 8-parameter approximation to the fixed point action[9] contain-

Table 1

Recent work on pure gauge system with improved actions. Argument for β_c means spatial volume, $\mu(L)$ the torelon mass for spatial size L and N_t the temporal lattice size.

action	ref.	measurements	N_t
<u>RG-improved</u>			
FP (type I)	[9]	$\beta_c(\infty), \mu(L)$	2, 3, 4, 6
FP (type IIIa)	[10]	$\beta_c(\infty)$	2, 3, 4, 6
FP (type IIIa)	[11]	p	2, 3
RG(1,2)	[12]	$\beta_c(\infty), \sigma$	4, 6
	[13]	$\beta_c(\infty), \mu(L)$	2, 3
<u>Symanzik-improved</u>			
S(1,2) _{tree}	[14]	$\beta_c(4N_t)$	3, 4, 5, 6
	[15]	$\beta_c(\infty), \sigma, \epsilon, p, \sigma_I$	4
S(1,2) _{tadpole}	[15]	$\beta_c(\infty), \sigma, \epsilon, p, \sigma_I$	4
S(2,2) _{tree}	[16,15]	$\beta_c(\infty), \sigma, \epsilon, p$	4
SLW _{tadpole}	[17]	$\beta_c(2N_t), \mu(L)$	2, 3, 4
	[13]	$\beta_c(\infty), \mu(L)$	2, 3

ing plaquette and unit parallelogram and their power up to 4; type I [9] and type IIIa [10] differ in the blocking procedure, the latter including 5 and 7 link staples to improve rotational symmetry. Actions improved according to Symanzik's program with the addition of an $m \times n$ loop are denoted as S(m,n), distinguishing tree-level coefficients from tadpole-improved ones[19] by corresponding suffices. The S(1,2) action improved to one loop order[20] including tadpole factors[21] is denoted by SLW_{tadpole}.

2.1. Critical temperature

2.1.1. $T_c/\sqrt{\sigma}$

A basic quantity for the pure gauge system is the ratio $T_c/\sqrt{\sigma}$, where σ is the string tension extracted from the static quark-antiquark potential. In Fig. 1 we plot recent results for this ratio for improved actions and the plaquette action[2] as a function of $(aT_c)^2 = 1/N_t^2$ with N_t the temporal lattice size. Results are not available for fixed point actions. For SLW_{tadpole}, for which values of σ are not given by the authors[17], we use an interpolation of the results reported in ref. [22].

Scaling behavior can be examined for two types of improved actions, SLW_{tadpole} and RG(1,2). Comparing their results with those of the pla-

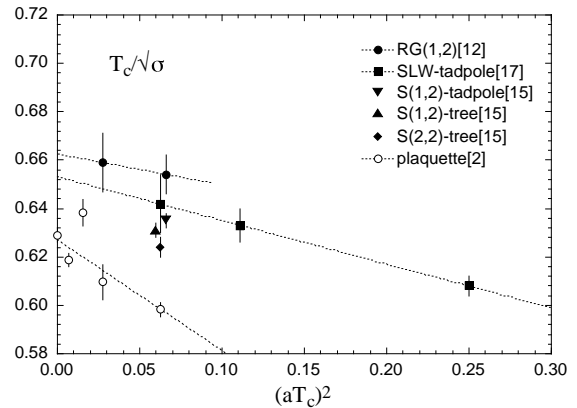


Figure 1. T_c for pure gauge system normalized by square root of string tension $\sqrt{\sigma}$ as a function of $(aT_c)^2$. Dotted lines are $O(a^2)$ fits.

quette action, it is apparent that the improved actions exhibit a better scaling behavior. For SLW_{tadpole} the ratio increases by about 5% over $aT_c \approx 0.25-0.5$, while a variation of 3–7% occurs for the plaquette action over a factor two smaller range $aT_c \approx 0.08-0.25$. The results for RG(1,2) are constant over $aT_c \approx 0.17-0.25$ within the quoted error of 1–2%. The errors are still sizable, however, to draw a conclusion on the magnitude of slope from the limited range of lattice spacing explored so far.

We observe, however, that the continuum extrapolation of $T_c/\sqrt{\sigma}$ for the improved actions do not agree with that for the plaquette action. For SLW_{tadpole}, assuming an $O(a^4)$ or $O(a^2)$ dependence (we ignore the factor g^4 of the actual form $O(g^4 a^2)$) both of which are consistent with present data, we find $T_c/\sqrt{\sigma} = 0.641(7)$ and $0.653(10)$ in the continuum limit. For RG(1,2) we expect an $O(a^2)$ scaling violation, with which we obtain $T_c/\sqrt{\sigma} = 0.663(13)$. These values are 2–5% (one to two standard deviations) larger compared to the estimate for the plaquette action $T_c/\sqrt{\sigma} = 0.629(3)$ [2] (open circle at $aT_c = 0$) obtained with a quadratic extrapolation.

We stress that efforts to resolve the discrepancy should be made for we would then have a determination of the basic ratio $T_c/\sqrt{\sigma}$ accurate at the level of 1–2%.

Let us add a remark on the results at

$aT_c = 0.25$ where values for six types of actions are available. Among those belonging to the category of Symanzik improvement, we observe that $T_c/\sqrt{\sigma}$ systematically increases in the order, plaquette \rightarrow $S(1,2)_{\text{tree}} \rightarrow S(1,2)_{\text{tadpole}} \rightarrow \text{SLW}_{\text{tadpole}}$, reaching $T_c/\sqrt{\sigma} \approx 0.64$. If we take $T_c/\sqrt{\sigma} \approx 0.65$ as the continuum value (see above), this trend is consistent with the theoretical expectation that cutoff effects are reduced with an increasing degree of improvement. In this regard $S(2,2)_{\text{tree}}$ seems less improved than $S(1,2)_{\text{tree}}$. The fact that the value for $\text{RG}(1,2)$ lies above that for $\text{SLW}_{\text{tadpole}}$ may be ascribed to a larger coefficient of the 1×2 loop term for this action compared to that for the latter.

2.1.2. $T_c/\sqrt{\sigma(L)}$

Another quantity often used for testing improvement with simulations on small lattices is the torelon mass $\mu(L)$ extracted from the Polyakov loop correlator on a lattice of spatial size L . Defining $\sigma(L) = \mu(L)/L$ we compile in Fig. 2 results for the ratio $T_c/\sqrt{\sigma(L)}$ for a fixed physical spatial size $L = 2/T_c$ as a function of $(aT_c)^2$. The results for the fixed point action FP (type I) and the plaquette action were already available last year [9] except for the value for the former for $N_t = 6$ [23]. This year, results have been reported for the actions $\text{SLW}_{\text{tadpole}}$ and $\text{RG}(1,2)$.

Taking all the data together, one finds a better scaling behavior exhibited by the improved actions compared to the plaquette action. On a closer look, however, some discrepancy is observed among data for improved actions. While results for FP (type I) [9] show a constant behavior in aT_c within the quoted error of 1–2%, those for $\text{SLW}_{\text{tadpole}}$ obtained by the Cornell group [17] exhibits an increase of 4% over $aT_c = 0.5 - 0.25$, and increasingly deviate from those of FP (type I) toward smaller lattice spacings. The results for $\text{RG}(1,2)$ lie in between those of the two actions. There is also a discrepancy among results from ref. [17] and [13], both for $\text{SLW}_{\text{tadpole}}$.

In order to extract the torelon mass, the Cornell group [17] employs a multi-state fit including excited states to a set of Polyakov loop correlators unsmearred or smeared at either source or sink, while a single state fit to a correlator smeared at

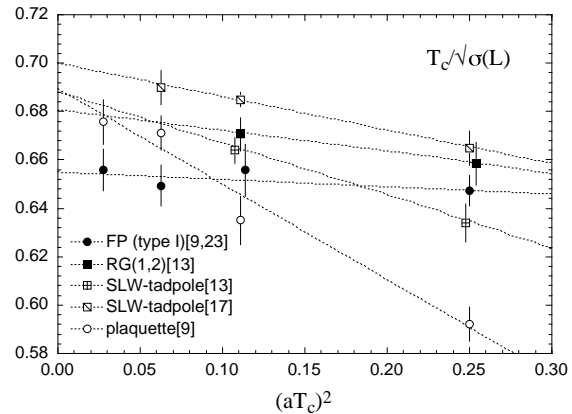


Figure 2. T_c normalized by $\sqrt{\sigma(L)}$ as a function of $(aT_c)^2$ where $\sigma(L) = \mu(L)/L$ with $\mu(L)$ the torelon mass for a physical spatial size L fixed at $L = 2/T_c$. Dotted lines are $O(a^2)$ fits.

source and sink is used in the other studies [9,13]. The discrepancy possibly originates from contamination of excited states in the latter fit [17].

Because of the different trend in the lattice spacing dependence, continuum extrapolation leads to a significant scatter of the ratio among the actions. Dotted lines in Fig. 2 illustrate the difference, where we assume $O(a^2)$ dependence since $O(a^2)$ terms are expected to be present for all the actions employed. Compared to the value for the plaquette action, the values for $\text{SLW}_{\text{tadpole}}$ and $\text{RG}(1,2)$ deviate at a $\pm(1-2)\%$ level, while that for FP (type I) is 6% lower.

The discrepancy should be resolved, particularly to ascertain if cutoff effects are reduced to within 1–2% at a large lattice spacing of $aT_c = 0.25 - 0.5$ for the fixed point action.

Another problem concerns the consistency between the values of $T_c/\sqrt{\sigma(L)}$ and $T_c/\sqrt{\sigma}$. The relation $\sigma \approx \sigma(L) + \pi/(3L^2)$ which holds in string models [24] suggests that $T_c/\sqrt{\sigma(L)}$ increases by about 0.04 compared to $T_c/\sqrt{\sigma}$ for $L = 2/T_c$. Making a comparison for each action, we find that the increase for $\text{SLW}_{\text{tadpole}}$ is consistent with this estimate. For the plaquette action the value of $T_c/\sqrt{\sigma(L)}$ in the continuum limit is 3% higher than the estimate, while for $\text{RG}(1,2)$ the value is 3% lower.

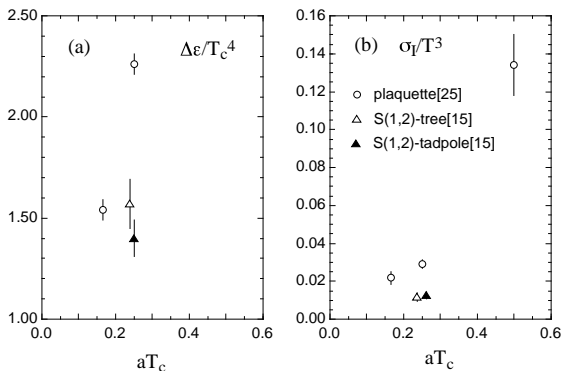


Figure 3. (a) latent heat $\Delta\epsilon/T_c^4$ and (b) interface tension σ_I/T_c^3 for plaquette[25] and Symanzik-improved S(1,2) action[15].

A systematic comparative analysis of various actions employing the same simulation and analysis procedures is needed to resolve this discrepancy.

2.2. Latent heat and interface tension

The latent heat $\Delta\epsilon$ and interface tension σ_I at the deconfinement transition exhibit large scaling violations from an $N_t = 4$ to an $N_t = 6$ lattice for the plaquette action as shown by open circles in Fig. 3. The Bielefeld group measured these quantities for the S(1,2) action[15] both without and with tadpole improvement (triangles).

For both quantities the rapid decrease of values for the plaquette action indicates that the continuum value would be lower than that on an $N_t = 6$ lattice. The values for the improved actions are indeed smaller already for $N_t = 4$.

2.3. Energy density and pressure

Bulk thermodynamic quantities such as energy density and pressure receive substantial contributions from high momentum modes. Since cutoff effects in these fluctuations are directly reduced by the improvement procedure, we may expect significant improvement.

Numerical tests have been made[15,16] for the actions S(1,2)_{tree}, tadpole and S(2,2)_{tree} through comparison of pressure calculated on an $N_t = 4$ lattice with an estimate of the continuum value obtained with the plaquette action[2]. The results for the improved actions are close to the continuum estimate already for $N_t = 4$, especially

for S(1,2)_{tadpole} for which a good agreement is seen even close to T_c . The fixed point action FP(type IIIa) also exhibits a similar agreement for $N_t = 3$ [11]. We refer to Figure 1 of ref. [15] for these points.

2.4. Summary

Improved actions lead to a sizable reduction of cutoff effects in thermodynamic quantities. Detailed scaling studies, however, are limited to that of critical temperature, for which consistency of results for various actions are not yet attained beyond the level of 5%. Further studies are needed to see if accurate determination of thermodynamic quantities at a few percent level is possible through simulations with a moderately large temporal size of $4 \leq N_t \leq 8$ with improved actions.

3. Chiral phase transition with the Kogut-Susskind quark action

3.1. Order of transition for $N_f = 2$

In Table 2 we list major studies on the order of two-flavor chiral phase transition carried out on an $N_t = 4$ lattice with the spatial size L^3 . In the finite-size scaling study pursued around 1989-1990[26,27], measurements were made of the susceptibility of the Polyakov line Ω given by

$$\chi_\Omega = L^3 [\langle (\text{Re}\Omega)^2 \rangle - \langle \text{Re}\Omega \rangle^2] \quad (1)$$

and a pseudo-susceptibility of chiral order parameter defined by

$$\chi_c = \frac{1}{9L^3} [\langle (\xi^\dagger D^{-1} \xi)^2 \rangle - \langle \xi^\dagger D^{-1} \xi \rangle^2] \quad (2)$$

where ξ is a gaussian noise and D the Kogut-Susskind quark operator. It was found that the peak height of the two susceptibilities increases

Table 2

Studies of order of $N_f = 2$ chiral transition on an $N_t = 4$ lattice.

	ref.	size	m_q
KEK(1990)	[26]	$6^3, 8^3, 12^3$	0.0125, 0.025
Columbia(1990)	[27]	16^3	0.01, 0.025
Bielefeld(1994)	[4]	8^3	0.02 – 0.075
Bielefeld(1996)	[28]	$12^3, 16^3$	0.02 – 0.075
JLQCD(1996)	[29]	$8^3, 12^3, 16^3$	0.01 – 0.075

up to 12^3 , but stays constant within errors between 12^3 and 16^3 both at $m_q = 0.025$ and $0.0125 - 0.01$ (see Fig. 11 and 12 in the second paper of ref. [27]). The saturation implies the absence of a phase transition down to $m_q \approx 0.01$. Since this quark mass is quite small, corresponding to $m_\pi/m_\rho \approx 0.2$ at the point of the transition $\beta_c \approx 5.27$, it was thought that the result is consistent with the transition being of second order at $m_q = 0$ as suggested by the sigma model analysis[5].

3.1.1. Scaling analysis of susceptibilities

One can attempt to examine if the transition is of second order employing the method of scaling analysis. Let us define the susceptibilities χ_m and $\chi_{t,i}$ ($i = f, \sigma, \tau$) by

$$\chi_m = V [\langle (\bar{q}q)^2 \rangle - \langle \bar{q}q \rangle^2] \quad (3)$$

$$\chi_{t,f} = V [\langle \bar{q}q \cdot \bar{q}D_0q \rangle - \langle \bar{q}q \rangle \langle \bar{q}D_0q \rangle] \quad (4)$$

$$\chi_{t,i} = V [\langle \bar{q}q \cdot P_i \rangle - \langle \bar{q}q \rangle \langle P_i \rangle], \quad i = \sigma, \tau \quad (5)$$

with $V = L^3 N_t$, D_0 the temporal component of the Dirac operator, and $P_{\sigma,\tau}$ the spatial and temporal plaquette. For a given quark mass m_q , let $g_c^{-2}(m_q)$ be the peak position of χ_m as a function of the coupling constant g^{-2} , and let χ_m^{max} and $\chi_{t,i}^{max}$ ($i = f, \sigma, \tau$) be the peak height. For a second-order transition, these quantities are expected to scale toward $m_q \rightarrow 0$ as

$$g_c^{-2}(m_q) = g_c^{-2}(0) + c_g m_q^{z_g} \quad (6)$$

$$\chi_m^{max} = c_m m_q^{-z_m} \quad (7)$$

$$\chi_{t,i}^{max} = c_{t,i} m_q^{-z_{t,i}}, \quad i = f, \sigma, \tau \quad (8)$$

Let us note that $\chi_{t,i}$ ($i = f, \sigma, \tau$) are three parts of the susceptibility $\chi_t = V [\langle \bar{q}q \cdot \epsilon \rangle - \langle \bar{q}q \rangle \langle \epsilon \rangle]$ with ϵ the energy density[4]. The leading exponent is therefore given by $z_t = \text{Max}(z_{t,f}, z_{t,\sigma}, z_{t,\tau})$.

Natural values to expect for the exponents z_g, z_m and z_t at a finite lattice spacing are those of $O(2) \approx U(1)$ corresponding to the exact symmetry group of the Kogut-Susskind action. However, sufficiently close to the continuum limit where flavor breaking effects are expected to disappear, they may take the values for $O(4) \approx SU(2) \otimes SU(2)$ which is the group of chiral symmetry for $N_f = 2$ in the continuum. One should also remember that mean-field exponents control

the scaling behavior not too close to the transition. A possibility of mean-field exponents arbitrarily close to the critical point has also been discussed[30].

The initial scaling study was carried out by Karsch and Laermann[4] employing an $8^3 \times 4$ lattice and $m_q = 0.02, 0.0375, 0.075$. Compared to the $O(4)$ values their results for exponents show a good agreement of z_m , a 50% larger value for z_g and a value twice larger for z_t . Comparison with $O(2)$ and mean-field exponents is similar since they are not too different from the $O(4)$ values.

This work had limitations in several respects: (i) the scaling formulae are valid for a spatial size large enough compared to the correlation length. At $m_q = 0.02$ the pion correlation length equals $\xi_\pi \approx 3$. Whether the spatial size of $L = 8$ employed is sufficiently large has to be examined. (ii) The size of the scaling region in terms of quark mass is *a priori* not known. Hence the behavior for smaller quark masses should be explored to check if the results are not affected by sub-leading and analytic terms in an expansion of susceptibilities in m_q . (iii) In the original work the noisy estimator with a single noise vector was employed to estimate disconnected double quark loop contributions. This introduces contamination from connected diagrams and local contact terms, which has to be removed. Other factors such as step size of the hybrid R algorithm and stopping condition for the solver of Kogut-Susskind matrix could also affect the value of susceptibilities.

For these reasons the Bielefeld group has continued their study[28], and the JLQCD Collaboration[29] has started their own work last year. As one sees in Table 2 run parameters of new simulations are chosen to examine the points (i) and (ii) above. In order to deal with (iii) Bielefeld group worked out the correction formula for the case of the single noise vector. They also employed the method of multiple noise vectors for some of the runs. JLQCD employed the method of wall source without gauge fixing[31], and removed contamination by a correction formula. At present both groups have accumulated $(5 - 10) \times 10^3$ trajectories of unit length with a small step size of $\delta\tau = (1 - 1/2)m_q$ for each

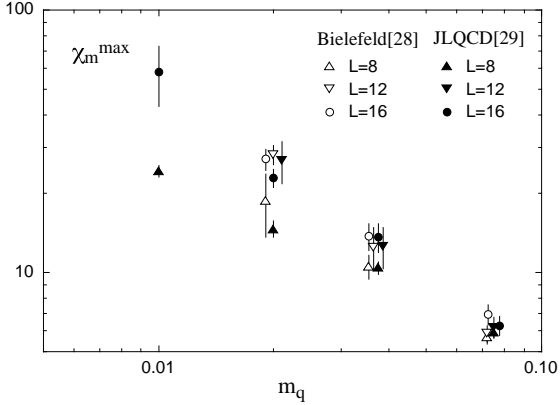


Figure 4. Peak height of χ_m as a function of m_q for spatial sizes $L = 8, 12, 16$.

value of β and m_q . The standard reweighting technique[32] is used to find the peak of susceptibilities.

In Fig. 4 we plot results of the two groups for the peak height of the chiral susceptibility χ_m for three spatial sizes $L = 8, 12$ and 16 . The two results are consistent. A striking feature in Fig. 4 is that, except for the largest quark mass $m_q = 0.075$, the peak height exhibits a significant size dependence whose magnitude rapidly increases toward small quark masses. In more detail, for $m_q = 0.0375$ and 0.02 , the increase is largest between $L = 8$ and 12 , while the peak height is consistent between $L = 12$ and 16 . At $m_q = 0.01$ the peak height increases by a factor 3 between $L = 8$ and 16 . Data on a 12^3 lattice is not yet available for this quark mass.

We should remark that the new data for $m_q = 0.01$ for $L = 16$ [29] do not agree with the previous results reported in ref. [27]. For the susceptibilities χ_c and χ_Ω for which a direct comparison is possible, new simulations give values which are a factor two larger than the old results. It is possible that a smaller statistics (2500 trajectories[27] as compared to 4400[29]), and perhaps also a slightly smaller estimate of the critical coupling ($\beta_c = 5.265$ as compared to $\beta_c = 5.266$), led to an underestimate of susceptibilities in ref. [27].

We list the exponents obtained through fits of form (6-8) in Table 3. While some systematic difference appears present for $z_{t,i}$ between the two groups, a significant increase of z_m and $z_{t,i}$ from

Table 3

Exponents for $N_f = 2$. For each exponent first row represents Bielefeld results[28] and second those of JLQCD[29]. Results are not yet available for entries marked with “-”.

	$O(2)$	$O(4)$	MF	$L=8$	$L=12$	$L=16$
z_g	0.60	0.54	2/3	0.77(14)	—	—
				0.70(10)	—	0.63(5)
z_m	0.79	0.79	2/3	0.79(4)	1.05(8)	0.93(9)
				0.70(3)	1.01(11)	1.02(7)
z_t	0.39	0.33	1/3			
$z_{t,f}$				0.65(7)	—	—
				0.42(4)	0.75(12)	0.78(8)
$z_{t,\sigma}$				0.63(7)	0.96(12)	0.86(11)
				0.48(4)	0.79(14)	0.81(9)
$z_{t,\tau}$				0.63(7)	0.94(13)	0.85(12)
				0.47(4)	0.81(14)	0.82(9)

$L = 8$ to $L = 12 - 16$ is evident, with the values for larger sizes sizably deviating from either $O(4), O(2)$ or the mean-field predictions. For z_g the deviation seems less apparent though full data are not yet available.

A puzzling nature of the values of exponents becomes clearer if we translate them into the more basic thermal and magnetic exponents y_t and y_h using the relations,

$$z_g = \frac{y_t}{y_h}, \quad z_m = \frac{d}{y_h}, \quad z_t = \frac{y_t}{y_h} + \frac{d}{y_h} - 1 \quad (9)$$

with $d = 3$ the space dimension. The values in Table 3 are reasonably consistent with the relation $z_g + z_m = z_t + 1$ which follow from (9). We observe that $z_m \approx 1.0(1)$ obtained for larger spatial lattices implies $y_h \approx 3.0(3)$ to be compared with the $O(4)$ value 2.49, while $y_h = d = 3$ is expected for a first-order phase transition. For the thermal exponent we find $y_t \approx 2.4(3)$ if we take $z_t \approx 0.8(1)$ or $y_t \approx 2.7(3)$ for $z_t \approx 0.9(1)$, which is substantially larger than the $O(4)$ value of 1.34.

One may think of various possibilities for the reason leading to these values of exponents. (i) The most conventional would be that the influence of sub-leading and analytic terms is still sizable at the range of quark mass explored. (ii) Another possibility, suggested by the value $y_h \approx d$ for $L = 12$ and 16 , is that a disconti-

nity fixed point with $y_h = d$ [33] controlling the first-order transition along the line $m_q = 0$ in the low-temperature phase is strongly influencing the scaling behavior. The transition is of second order in this case. Whether the deviation of y_t from any of the expected values can be explained is not clear, however. (iii) The transition is of second order with the exponents close to but not equal to d . This would mean a significant departure from the universality concepts, stepping even beyond the suggestion of mean-field exponents arbitrarily close to the critical point[30]. (iv) The transition is of first order. In this case, the value of quark mass $m_q = m_q^c$ at which the first-order transition terminates would have to be small or even vanish since the scaling formula is derived under the assumption of a transition taking place at a single point at $m_q = 0$.

Concerning the possibility (iv), results of present data examined from finite-size scaling point of view are as follows. As we already pointed out, χ_m for a fixed value of m_q stays constant for $L = 12 - 16$ down to $m_q = 0.02$. Results for other susceptibilities exhibit a similar behavior. Thus a phase transition does not exist for $m_q \geq 0.02$ as concluded in the previous studies[26,27]. At $m_q = 0.01$ the susceptibilities increase by a factor 3 between $L = 8$ and 16. Runs for $L = 12$ are needed to see if the increase is consistent with a linear behavior in volume expected for a first-order transition.

We have to conclude that scaling analyses of susceptibilities carried out so far do not allow a definite conclusion. Much further work, possibly with a quark mass smaller than has been explored so far, is needed to elucidate the nature of the chiral transition for $N_f = 2$.

3.1.2. Scaling analysis of chiral order parameter

For a second-order transition the singular part of the chiral order parameter is expected to scale as $\langle \bar{q}q \rangle = m_q^{1/\delta} \phi(x)$ where $\phi(x)$ is a function of the scaling variable $x = (g^{-2} - g_c^{-2}(0))/m_q^{1/\beta\delta}$, and $1/\delta = 1 - d/y_h$ and $1/\beta\delta = y_h/y_t$. A previous analysis[34] employing a collection of data generated over the years did not find clear sign of scaling with the $O(4)$ exponents. This year

the MILC Collaboration attempted a more elaborate analysis as part of their study of equation of state[35].

For systems in the $O(4)$ universality class, the scaling function $\phi(x)$ may be determined in a parameterized form through a simulation of the $O(4)$ sigma model up to an overall constant for the scaling variable x [36]. The result for $\phi(x)$ is used to fit data for $\langle \bar{q}q \rangle$ generated on a $12^3 \times 6$ lattice with $m_q = 0.025$ and 0.0125 . Adding an analytic term of form $m_q(c_0 + c_1/g^2 + c_2/g^4)$, the fit was found acceptable for $O(4)$ and also for the mean-field scaling function. Extrapolating to the limit $m_q = 0$, the results differ significantly between the two cases, however (see Fig. 2 of ref. [35]).

We note that the results of the present MILC analysis do not contradict those of susceptibilities: the quark mass used for this work corresponds to $m_q \approx 0.02 - 0.04$ on an $8^3 \times 4$ lattice, for which case the exponents found from susceptibilities are similar to the $O(4)$ values. We further remind, however, that the exponents exhibit a significant size dependence. This means that studies with larger lattice sizes and smaller m_q are required to explore the nature of the two-flavor transition from scaling of the chiral order parameter.

3.2. Restoration of $U_A(1)$ symmetry

For sufficiently high temperatures topologically non-trivial gauge configurations are suppressed, leading to restoration of $U_A(1)$ symmetry. To what extent $U_A(1)$ symmetry is restored close to the chiral transition is an interesting question.

Three groups[35,37,28] examined the problem using the susceptibility defined by

$$\chi_{U_A(1)} = \int d^4x (\langle \vec{\pi}(x) \cdot \vec{\pi}(0) \rangle - \langle \vec{a}_0(x) \cdot \vec{a}_0(0) \rangle) \quad (10)$$

which should vanish at $m_q = 0$ if $U_A(1)$ symmetry is restored. In Fig. 5 we plot the m_q dependence of this quantity obtained by the MILC Collaboration[35] and the Columbia group[37]. Both results are taken in the high temperature phase corresponding to $T/T_c \approx 1.2 - 1.3$. While the data appear to extrapolate linearly to zero at $m_q = 0$ (dotted lines)[37], it is more reason-

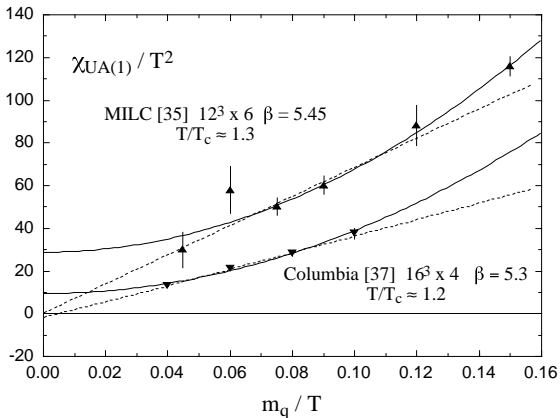


Figure 5. Susceptibility for $U_A(1)$ symmetry as a function of m_q/T .

able to fit with a quadratic dependence $\chi_{U_A(1)} = a + bm_q^2 + O(m_q^4)$ (solid lines)[35] since the susceptibility is expected to be an analytic function of m_q and hence even in m_q in the high temperature phase. These fits, which have reasonable χ^2 , lead to a non-zero value of $\chi_{U_A(1)}$ at $m_q = 0$. Thus effect of anomaly still breaks $U_A(1)$ symmetry just above the chiral transition. Similar results were reported in ref. [28].

The Illinois group[38] calculated the screening mass of σ, π, a_0 on a $16^3 \times 8$ lattice at $m_q = 0.00625$, employing a noisy estimator for the disconnected contribution for the σ propagator. They found a decrease of the mass splitting $m_\pi - m_{a_0}$ across the transition, which, however, remains at the level of 20% just above T_c for the quark mass employed. They have also shown that the disconnected part of the σ propagator is dominated by fermionic modes with small eigenvalues induced by instantons. The latter results parallel those of a previous study carried out for the quenched Wilson case[39].

3.3. Energy density and pressure

The MILC Collaboration completed their study of equation of state for the temporal size $N_t = 6$ [35], following their previous work for $N_t = 4$ [40]. They also attempted an extrapolation of equation of state toward $m_q \rightarrow 0$ making use of the scaling function computed for the chiral order parameter.

The Bielefeld group[15] made a measurement of

energy density for $N_f = 4$ employing the three-link improved form of the Kogut-Susskind action[41] together with $S(1,2)_{\text{tree}}$ for the gauge action.

In the results of both groups the energy density ϵ/T^4 rapidly rises across T_c and stays close to the continuum Stefan-Boltzmann value in the high temperature phase. In the MILC result a bump just above T_c seen for $N_t = 4$ almost disappears for $N_t = 6$. A similar bump, while observed by the Bielefeld group at finite m_q in their $N_f = 4$ results, is no longer present if terms vanishing in the chiral limit is removed.

These results indicate that ϵ/T^4 for full QCD is a monotonically increasing function of temperature similar in shape to that of the pure gauge system[2]. The behavior of pressure $3p/T^4$ is also similar, rising smoothly from $T \approx T_c$ and reaching ϵ/T^4 at $T/T_c \approx 2 - 3$.

4. Phase structure for the Wilson quark action

4.1. Previous phase diagram studies

A basic concept in the phase structure analysis for the Wilson quark action is that of the critical line $K = K_c(\beta)$ which is usually defined as the line of vanishing pion mass. At zero temperature this line runs from $K \approx 1/4$ at $\beta = 0$ to $K = 1/8$ at $\beta = \infty$, and chiral symmetry is expected to become restored toward the weak-coupling limit along this line[42].

At finite temperatures there also exists the line of finite-temperature transition $K = K_t(\beta)$, the thermal line. This line starts from the point of the deconfinement transition of the pure gauge system at $K = 0$, and moves toward the critical line. Naively one would expect the thermal line to hit the critical line at some finite $\beta = \beta_{ct}$, separating the physical region $K \leq K_c(\beta)$ into low and high temperature phases.

Extensive studies have been carried out to examine if this expectation is realized[43–49]. A conceptual issue that arose in the course of studies is whether one can naturally define the critical line in the high temperature phase since pion mass does not vanish in this phase.

The QCDPAX Collaboration took the view[48]

that the critical line should be defined by the vanishing of the quark mass m_q at zero temperature, where m_q is defined through chiral Ward identity[42,50,51]. They reported that the crossing point β_{ct} with this definition of the critical line is located in the region of strong coupling on an $N_t = 4$ lattice, *e.g.*, $\beta_{ct} \approx 3.9 - 4.0$ for $N_f = 2$. For the phase diagram based on this result see ref. [6].

This phase diagram, however, has an unsatisfactory feature. It has been observed[48,49] that physical observables do not exhibit any singular behavior across the critical line in the high temperature phase. This means that the region $K \geq K_c(\beta)$, usually thought unphysical, is not distinct from the high temperature phase, being analytically connected to it. Hence one can cross from the low- to the high-temperature phase through the part of the critical line below $\beta = \beta_{ct}$, which is not a line of finite-temperature transition.

Clearly the phase diagram above does not capture the full aspect of the phase structure. Recent investigations indicate that a more natural understanding of the phase structure is provided by a different view on the critical line proposed by Aoki some time ago[7]. In the following we review the phase structure based on this view.

Let us note that a slightly different phase structure has been discussed in ref. [52]. The phase structure for general values of N_f up to $N_f = 300$ has also been examined recently[53].

4.2. Spontaneous breakdown of parity-flavor symmetry and massless pion

In order to illustrate the basic idea, let us consider an effective sigma model for lattice QCD with the Wilson quark action with $N_f = 2$. The effective lagrangian may be written as

$$\mathcal{L}_{eff} = (\nabla_\mu \vec{\pi})^2 + (\nabla_\mu \sigma)^2 + a\vec{\pi}^2 + b\sigma^2 + \dots \quad (11)$$

where the coefficients a and b differ reflecting explicit breaking of chiral symmetry due to the Wilson term. We know that the pion mass vanishes as $a = m_\pi^2 \propto K_c - K$ toward the critical line, while σ stays massive, *i.e.*, $b = m_\sigma^2 > 0$ at $K \approx K_c$. If K increases beyond K_c , the coefficient a becomes negative. Hence we expect the pion field to de-

velop a vacuum expectation value $\langle \vec{\pi} \rangle \neq 0$. The condensate spontaneously breaks parity and flavor symmetry.

Let us note that pion is not the Nambu-Goldstone boson of spontaneously broken chiral symmetry in this view. Instead it represents the massless mode of a parity-flavor breaking second-order phase transition which takes place at $K = K_c$. We expect it to become the Nambu-Goldstone boson of chiral symmetry in the continuum limit, however, as chiral symmetry breaking effects disappear in this limit.

The idea above has been explicitly tested for the two-dimensional Gross-Neveu model formulated with the Wilson action[7]. An analytic solution in the large N limit shows spontaneous breakdown of parity for $K \geq K_c(\beta)$. Another important result of the solution is that the critical line forms three spikes, which reach the weak-coupling limit $g = 0$ at $1/2K = +2, 0, -2$. This structure arises from the fact that the doublers at the conventional continuum limit $(g, 1/2K) = (0, 2)$ become physical massless modes at $1/2K = 0$ and -2 .

A close similarity of the Gross-Neveu model and QCD regarding the asymptotic freedom and chiral symmetry aspects leads one to expect a similar phase structure for the case of QCD except that the critical line will form five spikes reaching the continuum limit because of difference in dimensions[7]. Evidence supporting such a phase structure is summarized in ref. [54].

4.3. Finite-temperature phase structure

For a finite temporal lattice size N_t corresponding to a finite temperature, the above consideration can be naturally extend by defining the critical line as the line of vanishing pion screening mass determined from the pion propagator for large spatial separations.

In Fig. 6 the critical line for the two-dimensional Gross-Neveu model calculated in the large N limit is plotted for $N_t = \infty, 16, 8, 4, 2$ starting from the outermost curve and moving toward inside. The result shows that the location of the critical line as defined above depends on N_t . Another important point is that the spikes formed by the critical line moves away from the

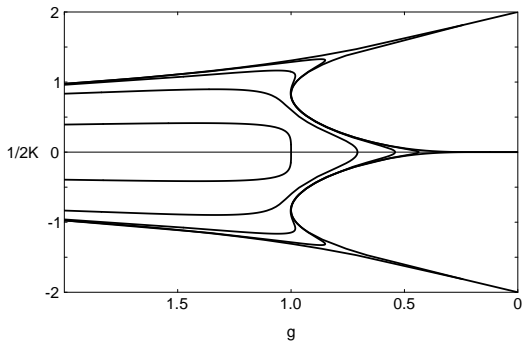


Figure 6. Critical line in $(g, 1/2K)$ plane for the two-dimensional Gross-Neveu model for the temporal size $N_t = \infty, 16, 8, 4, 2$ (from outside to inside) [55].

weak-coupling limit as N_t decreases.

Simulations to examine if lattice QCD has a similar structure of the critical line at finite temperatures have been made recently for the case of $N_f = 2$ [55] and 4 [56] on an $8^3 \times 4$ lattice. The results are summarized as follows: (i) For both systems the conventional critical line turns back toward strong coupling forming a cusp, whose tip is located at $\beta \approx 4.0$ for $N_f = 2$ and $\beta \approx 1.8$ for $N_f = 4$. The cusp represents one of five cusps expected for lattice QCD. (ii) Parity and flavor symmetry are spontaneously broken inside the cusp. Simulations have been made for the $N_f = 2$ system with an external field term $\delta S_W = 2KH \sum_n \bar{\psi}_n i\gamma_5 \tau_3 \psi_n$ added to the action. Results provide evidence for the behavior $\lim_{H \rightarrow 0} \langle \bar{\psi} \gamma_5 \tau_3 \psi \rangle \neq 0$ of the parity-flavor order parameter and vanishing of π^\pm mass $\lim_{H \rightarrow 0} m_{\pi^\pm} = 0$ expected inside the cusp [56].

Concerning the relation between the thermal line and the critical line, we recall that the pion mass vanishes all along the critical line. This suggests that the region close to the critical line is in the cold phase even after the critical line turns back toward strong coupling, and hence the thermal line cannot cross the critical line. Since numerical estimates show that the thermal line comes close to the turning point of the cusp, the natural possibility is that the thermal line runs past the tip of the cusp and continues toward larger values of K . Results of measurement of thermodynamic quantities provide support of this

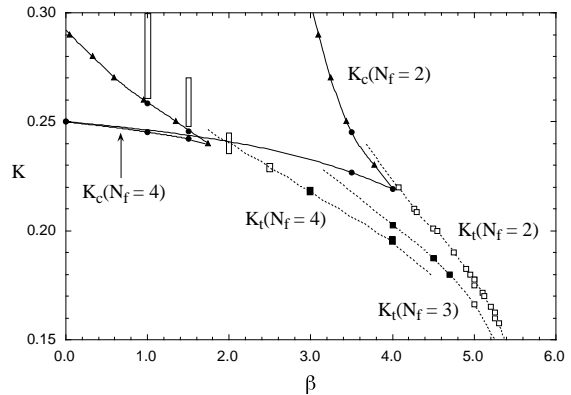


Figure 7. Phase diagram for $N_f = 2, 3, 4$ on an $N_t = 4$ lattice.

view [55], although the possibility that the thermal line touches the critical line at a point [48] cannot be excluded.

In Fig. 7 we summarize presently available results for the phase structure on an $N_t = 4$ lattice for $N_f = 2, 3$ and 4. Solid lines represent the critical line estimated from the pion mass. For the case of $N_f = 3$ results confirming the cusp structure are not yet available. Open and solid squares show simulation results for the location of the thermal line. Dotted lines are smooth interpolation, extended beyond the cusp following the discussion of the previous paragraph. The difference of open and solid squares is discussed in Sec. 4.4 below.

Let us remark that the conventional zero temperature critical line runs close to the lower part of the finite-temperature critical line in Fig. 7 and continues toward weak coupling. The thermal line therefore has to cross the zero-temperature critical line. This represents the crossing point β_{ct} reported by the QC DPAX Collaboration [48].

We emphasize, however, that the zero-temperature critical line does not represent a line of singularity of the finite-temperature partition function. This naturally explains the absence of singular behavior of observables across the zero-temperature critical line mentioned in Sec. 4.1.

4.4. N_f dependence of order of transition

The sigma model analysis in the continuum [5] suggests that the chiral phase transition is of second order for $N_f = 2$ and of first order for $N_f \geq 3$.

Indeed strong first-order signals have been observed for the case of $N_f = 3$ [48] and 4[56] away from the critical line, as shown by solid squares in Fig. 7, in contrast to a crossover behavior represented by open squares seen for $N_f = 2$. However, the first-order transition for $N_f = 4$ weakens closer to the critical line, apparently turning into a smooth crossover before reaching the region around the cusp of the critical line as indicated by open rectangles[56]. While parallel data are not yet available for $N_f = 3$, results of the QCD-PAX Collaboration[48] also appears to indicate a weakening of the first-order transition.

A possible reason for this unexpected behavior is that breaking of chiral symmetry due to the Wilson term, which becomes stronger as β decreases along the thermal line, smoothens the first-order transition. Another possibility is that the first-order transition for $N_f = 3$ and 4 observed so far is a lattice artifact sharing its origin with the sharpening of the crossover at $\beta \approx 5.0$ found by the MILC Collaboration for $N_f = 2$ [49]. Some support for this interpretation is given by a recent study of the QCDPAX Collaboration for the $N_f = 3$ system with an improved gauge action[57]. So far they have not found clear first-order signals in the region where the plaquette action shows a clear first-order behavior.

In either case, if chiral transition in the continuum is indeed of first order for $N_f = 3$ and 4, it will emerge only when the cusp moves sufficiently toward weak-coupling with an increase of the temporal size N_t .

4.5. Continuum limit

We expect the cusp of the finite-temperature critical line to grow toward weak coupling as N_t increases. In the limit $N_t = \infty$ it should converge to the zero-temperature critical line which reaches $\beta = \infty$. Since the thermal line is located on the weak-coupling side of the cusp for a finite N_t , it will be pinched by the tip of the cusp at $(\beta, K) = (\infty, 1/8)$ as $N_t \rightarrow \infty$. We expect chiral phase transition in the continuum to emerge in this limit. In order to extract continuum properties of the chiral transition, we then need a systematic study of thermodynamic quantities in the neighborhood of the thermal line when it runs

close to the tip of the cusp as a function of N_t .

Simulations, however, indicate that the cusp moves only very slowly as N_t increases. For the $N_f = 2$ case, current estimates of the position of the tip of the cusp is $\beta \approx 4.0$ for $N_t = 4$ [55], $4.0 - 4.2$ for $N_t = 6$ [48], $4.2 - 4.3$ for $N_t = 8$ [56] and $4.5 - 5.0$ even for $N_t = 18$ [48]. A recent work also reports an absence of parity-broken phase above $\beta = 5.0$ on symmetric lattices up to the size 10^4 [60]. For $N_f = 4$ the values are even lower: $\beta \approx 1.80$ for $N_t = 4$ and $2.2 - 2.3$ for $N_t = 8$ [56]. These estimates indicate that a very large temporal size will be needed for the cusp to move into the scaling region (*e.g.*, $\beta \geq 5.5$ for $N_f = 2$) as long as one employs the Wilson quark action together with the plaquette action for the gauge part.

We emphasize that this result has an important implication also for spectrum calculations at zero temperature. Since the location of the cusp is determined by the smaller of the spatial and temporal size, the critical line will be shifted or may even be absent unless lattice size is taken sufficiently large. Therefore hadron masses calculated on a lattice of small spatial size and extrapolated toward the position of the critical line might involve significant systematic uncertainties.

4.6. Studies with improved actions

The problems discussed above indicate the presence of sizable cutoff effects when the Wilson quark action is used in conjunction with the plaquette action. A way to alleviate this problem is to employ improved actions. This approach has been pursued by the QCDPAX Collaboration[8,57], replacing the plaquette action with an improved gauge action RG(1,2)[18]. This year the MILC Collaboration reported simulations with the action $SLW_{tadpole}$ for the gauge part and the tadpole-improved clover action for the quark part[58]. Results with the tree-level clover action keeping the plaquette action are also available[59]. Thus there are data for four types of action combinations, unimproved and improved both for the gauge and quark actions, to make a comparative study of improvement.

An indication from such a comparison is that improving the gauge action substantially removes

cutoff effects. An inflection of the critical line seen for the plaquette action at $\beta \approx 4 - 5$ becomes absent with improvement of the gauge action[8], while it still seems to remain if only the Wilson quark action is replaced by the clover action[59]. Also an intermediate sharpening of the thermal transition seen for the plaquette action at $\beta \approx 5.0$ [49] is not observed for improved actions[8,58].

Another point to note is that the lattice spacing at the coupling constant where the thermal line approaches the critical line has a similar value $m_\rho a \approx 1$ on an $N_t = 4$ lattice for all of the four action combinations. This means that studies of physical quantities are needed to assess reduction of cutoff effects with improved actions. Interesting results have already been obtained for scaling of the chiral order parameter[8,61], and work with the critical temperature is being pursued[8,58].

5. Results in finite density studies

It has long been known that the quenched approximation breaks down for a non-zero quark chemical potential μ in that a transition takes place at $\mu \approx m_\pi/2$ rather than at $\mu \approx m_N/3$ [62, 63]. While the importance of the phase of the quark determinant has been made clear, the mechanism how the quenched approximation breaks has not been fully explained.

Recently Stephanov[64], employing a random matrix model of the quark determinant[65] and a replica formulation of quenched approximation, traced back the failure of the quenched approximation to the non-uniformity of the limit of the replica number $n \rightarrow 0$ for $\mu = 0$ and $\mu > 0$. He has also shown that the quenched approximation is valid for the theory in which a quark χ in the conjugate representation is added to each quark q . Formation of a condensate $\langle \bar{\chi}q \rangle$ having a unit baryon number and a mass $m_{\bar{\chi}q} \approx m_\pi$ in such a theory explains the occurrence of transition at $\mu \approx m_\pi/2$.

Barbour and collaborators reported new results in full QCD simulations[66]. With the method of fugacity expansion[67] runs were carried out for four flavors of quarks on 6^4 and 8^4 lattices at $\beta = 5.1$ with the Kogut-Susskind quark action. They found an onset of non-zero baryon number

at a small value of μ , *e.g.*, $\mu_c \approx 0.1$ at $m_q = 0.01$. For comparison the MT_c Collaboration reported $m_N = 1.10(6)$ and $m_\pi = 0.290(6)$ at a slightly larger coupling of $\beta = 5.15$ at $m_q = 0.01$ [68].

It is not yet clear if these results mean that an early onset of transition $\mu_c \approx m_\pi/2$ also holds for full QCD or reflect computational problems of the method employed for the simulation.

6. Conclusions

Much work has been made in finite temperature studies of lattice QCD encompassing a number of subjects during the last year.

Tests of improved actions made for the pure gauge system indicate a possibility that accurate results for thermodynamics in the continuum may be obtained with simulations carried out with a moderately large temporal size.

In full QCD studies much progress has been made in understanding the phase structure for the Wilson quark action. On the other hand, new problems have also been encountered, making it necessary to reexamine conclusions reached in previous studies. These are the unexpected values of exponents for $N_f = 2$ found in scaling studies of susceptibilities with the Kogut-Susskind quark action, and the flavor dependence of order of chiral transition with the Wilson quark action. Elucidating these problems is important for reaching an understanding of the nature of chiral phase transition, which is consistent between the Kogut-Susskind and Wilson quark actions.

Some progress has been made in QCD at finite density. A puzzling result reported from the latest simulation shows, however, that we are still far from understanding this difficult subject.

In closing we point out that most work in full QCD during the past several years have concentrated on the case of N_f degenerate quarks, especially for $N_f = 2$. While a variety of basic problems we have encountered for this case has to be clarified with further work, we should also recall that nature corresponds to the case of $N_f = 2 + 1$ with a heavier strange quark. A delicate change of phase that might possibly result from its presence, as suggested in the continuum sigma model analysis[5], makes it important to enlarge previ-

ous studies[27,69,48] into a systematic effort in this direction.

Acknowledgements

I would like to thank S. Aoki, F. Beinlich, T. Blum, W. Bock, G. Boyd, M. Creutz, N. Christ, T. DeGrand, C. DeTar, M. Fukugita, Y. Iwasaki, K. Kanaya, T. Kaneko, F. Karsch, E. Laermann, P. Mackenzie, M. Okawa, D. Tous-saint, M. Wingate and Y. Yoshié for communicating their results and for discussions. I would also like to thank S. Aoki, M. Fukugita, Y. Iwasaki, K. Kanaya and M. Okawa for comments on the manuscript. This work is supported in part by the Grant-in-Aid of the Ministry of Education, Science and Culture (Nos. 04NP0801, 08640349).

REFERENCES

1. For a review and references, see, A. Ukawa, *Lattice 89*, Nucl. Phys. B (Proc. Suppl.) 17 (1990) 118.
2. For a representative work, see, G. Boyd, J. Engels, F. Karsch, E. Laermann, C. Legeland, M. Lütgemeier and B. Petersson, Nucl. Phys. B469 (1996) 419.
3. For a summary as of 1990, see, S. Gottlieb, *Lattice 90*, Nucl. Phys. B (Proc. Suppl.) 20 (1991) 247.
4. F. Karsch, Phys. Rev. D49 (1993) 3791; F. Karsch and E. Laermann, Phys. Rev. D50 (1994) 6954.
5. R. D. Pisarski and F. Wilczek, Phys. Rev. D29 (1984) 338; F. Wilczek, Int. J. Mod. Phys. A7 (1992) 3911; K. Rajagopal and F. Wilczek, Nucl. Phys. B399 (1993) 395.
6. For previous reviews, see, Y. Iwasaki, *Lattice 94*, Nucl. Phys. B (Proc. Suppl.) 42 (1995) 96; K. Kanaya, *Lattice 95*, Nucl. Phys. B (Proc. Suppl.) 47 (1996) 144.
7. S. Aoki, Phys. Rev. D30 (1984) 2653; Phys. Rev. Lett. 57 (1986) 3136; Nucl. Phys. B314 (1989) 79.
8. Y. Iwasaki, K. Kanaya, K. Kaya, S. Sakai and T. Yoshié, *Lattice 94*, Nucl. Phys. B (Proc. Suppl.) 42 (1995) 502; *Lattice 95*, Nucl. Phys. B (Proc. Suppl.) 47 (1996) 515.
9. T. DeGrand, A. Hasenfratz, P. Hasenfratz and F. Niedermeyer, Nucl. Phys. B454 (1995) 587, 615.
10. M. Blatter and F. Niedermeyer, BUTP-96/12 (hep-lat/9605017).
11. A. Papa, BUTP-96/13 (hep-lat/9605004).
12. Y. Iwasaki *et al.* (presented by T. Kaneko), this volume, UTHEP-341 (hep-lat/9608090)
13. W. Bock, this volume (hep-lat/9608103); W. Bock, Y. Iwasaki, K. Kanaya and Yoshié, in preparation.
14. G. Cella, G. Curci, A. Viceré and B. Vigna, Phys. Lett. B333 (1994) 457.
15. F. Karsch, this volume, BI-TP 96/34 (hep-lat/9608047).
16. F. Beinlich, F. Karsch and E. Laermann, Nucl. Phys. B462 (1996) 415.
17. D. W. Bliss, K. Hornbostel and G. P. Lepage, SMUHEP 96-05 (hep-lat/9605041).
18. Y. Iwasaki, Nucl. Phys. B258 (1985) 141; Tsukuba preprint UTHEP-118 (1983), unpublished.
19. G. P. Lepage and P. Mackenzie, Phys. Rev. D48 (1993) 2250.
20. M. Lüscher and P. Weisz, Phys. Lett. B158 (1985) 250 and references therein.
21. M. Alford, W. Dimm, G. P. Lepage, G. Hockney and P. Mackenzie, Phys. Lett. B361 (1995) 87.
22. S. Collins, R. Edwards, U. Heller and J. Sloan, this volume (hep-lat/9608021).
23. T. DeGrand, private communication.
24. P. de Forcrand, G. Schierholz, H. Schneider and M. Teper, Phys. Lett. B160 (1985) 137.
25. Y. Iwasaki *et al.*, Phys. Rev. D46 (1992) 4657; Phys. Rev. D49 (1994) 3540; Y. Aoki and K. Kanaya, Phys. Rev. D50 (1994) 6921.
26. M. Fukugita, H. Mino, M. Okawa and A. Ukawa, Phys. Rev. Lett. 65 (1990) 816; Phys. Rev. D42 (1990) 2936.
27. F. R. Brown, F. P. Butler, H. Chen, N. H. Christ, Z. -H. Dong, W. Schaffer, L. I. Unger and A. Vaccarino, Phys. Rev. Lett. 65 (1990) 2491; A. Vaccarino, *Lattice 90*, Nucl. Phys. B (Proc. Suppl.) 20 (1991) 263.
28. G. Boyd, F. Karsch, E. Laermann and M. Oevers, BI-TP 96/27 (hep-lat/9607046); in progress (private communication from F.

- Karsch and E. Laermann).
29. JLQCD Collaboration, S. Aoki *et al.*, in progress.
 30. A. Kocić and J. B. Kogut, Phys. Rev. Lett. 74 (1995) 3109; Nucl. Phys. B455 (1995) 229.
 31. Y. Kuramashi *et al.*, Phys. Rev. Lett. 72 (1994) 3448.
 32. I. R. McDonald and K. Singer, Disc. Faraday Soc. 43 (1967) 40; A. M. Ferrenberg and R. Swendsen, Phys. Rev. Lett. 61 (1988) 2635.
 33. B. Nienhuis and M. Nauenberg, Phys. Rev. Lett. 35 (1975) 477.
 34. C. DeTar, *Lattice 94*, Nucl. Phys. B (Proc. Suppl.) 42 (1995) 73.
 35. MILC Collaboration (presented by C. Detar and T. Blum), this volume (hep-lat/9608026).
 36. D. Toussaint, AZPH-TH/96-13 (hep-lat/9607084)
 37. N. Christ, this volume.
 38. J. Kogut, J.-F. Lagaë and D. Sinclair, this volume, ANL-HEP-CP-96-52 (hep-lat/9608128).
 39. S. Itoh, Y. Iwasaki and Y. Yoshié, Phys. Rev. D36 (1987) 527.
 40. T. Blum, S. Gottlieb, L. Kärkkäinen and D. Toussaint, Phys. Rev. D51 (1995) 5153.
 41. S. Naik, Nucl. Phys. B316 (1989) 238.
 42. M. Bochicchio, L. Maiani, G. Martinelli, G. Rossi and M. Testa, Nucl. Phys. B262 (1985) 331.
 43. M. Fukugita, S. Ohta and A. Ukawa, Phys. Rev. Lett. 57 (1986) 1974.
 44. A. Ukawa, *Lattice 88*, Nucl. Phys. B (Proc. Suppl.) 9 (1989) 463.
 45. R. Gupta, A. Patel, C. Baillie, G. Guralnik, G. Kilcup and S. Sharpe, Phys. Rev. D40 (1989) 2072.
 46. K. M. Bitar, A. D. Kennedy and P. Rossi, Phys. Lett. B234 (1990) 333.
 47. HEMCGC Collaboration, K. M. Bitar *et al.*, Phys. Rev. D43 (1991) 2396.
 48. Y. Iwasaki *et al.*, Phys. Rev. Lett. 67 (1991) 1491; Phys. Rev. Lett. 69 (1992) 21; UTHEP-300(hep-lat/9504019); UTHEP-304(hep-lat/9505017). A full account is reported in, UTHEP-334(hep-lat/9605030).
 49. C. Bernard, M. Ogilvie, T. A. DeGrand, C. DeTar, S. Gottlieb, A. Krasnitz, R. L. Sugar and D. Toussaint, Phys. Rev. D46 (1992) 4741; C. Bernard *et al.* Phys. Rev. D49 (1994) 3574; *Lattice 93*, Nucl. Phys. B (Proc. Suppl.) 34 (1994) 324; T. Blum *et al.*, Phys. Rev. D50 (1994) 3377; C. Bernard *et al.*, *Lattice 94*, Nucl. Phys. B (Proc. Suppl.) 42 (1995) 451.
 50. S. Itoh, Y. Iwasaki, Y. Oyanagi and T. Yoshié, Nucl. Phys. B274 (1986) 33.
 51. L. Maiani and G. Martinelli, Phys. Lett. B178 (1986) 265.
 52. M. Creutz, hep-lat/9608024.
 53. Y. Iwasaki *et al.*, (presented by K. Kanaya and S. Kaya), this volume (hep-lat-9608125).
 54. S. Aoki, Prog. Theor. Phys. 122 (1996) 179 and references cited therein.
 55. S. Aoki, A. Ukawa and T. Umemura, Phys. Rev. Lett. 76 (1996) 873; *Lattice 95*, Nucl. Phys. B (Proc. Suppl.) 47 (1996) 511.
 56. S. Aoki, T. Kaneda, A. Ukawa and T. Umemura, this volume.
 57. Y. Iwasaki *et al.*, in progress.
 58. MILC Collaboration (presented by M. Wingate), this volume (hep-lat/9607085).
 59. S. Aoki, U. Ukawa and T. Umemura, unpublished (1995).
 60. K. M. Bitar, hep-lat/9602027.
 61. Y. Iwasaki *et al.*, UTHEP-344 (hep-lat/9609022).
 62. I. Barbour *et al.*, Nucl. Phys. B275[FS17] (1986) 296.
 63. M. -P. Lombardo, J. B. Kogut and D. Sinclair, Phys. Rev. D54 (1996) 2303 and references cited therein.
 64. M. A. Stephanov, Phys. Rev. Lett. 76 (1996) 4472; this volume (hep-lat/9607060).
 65. E. V. Shuryak and J. J. M. Verbaarschot, Nucl. Phys. A560 (1993) 306.
 66. I. M. Barbour, J. B. Kogut and S. E. Morrison (presented by S. E. Morrison), this volume (hep-lat/9608057).
 67. I. M. Barbour and Z. Sabeur, Nucl. Phys. B342 (1990) 269.
 68. MT_c Collaboration, R. Altmeyer *et al.*, Nucl. Phys. B389 (1993) 445.
 69. J. B. Kogut and D. K. Sinclair, Phys. Lett. B263 (1991) 101.